LIGHT ACTIVATES ROTATIONS OF BACTERIORHODOPSIN IN THE PURPLE MEMBRANE

PATRICK L. AHL AND RICHARD A. CONE
Thomas C. Jenkins Department of Biophysics, The Johns Hopkins University, Baltimore, Maryland 21218

ABSTRACT To investigate how a photoactivated chromophore drives the proton pump mechanism of bacteriorhodopsin, we have observed how the chromophore rotates during the photocyle. To do this, we examined the dichroism induced in aqueous suspensions of purple membrane fragments by flashes of linearly polarized light. We find that the flash stimulates both the photocycling chromophores and their noncycling neighbors to undergo large (>10°–20°) rotations within the membrane during the photocycle, and that these two chromophore populations undergo distinctly different sequences of rotations. All these rotations could be eliminated by glutaraldehyde fixation as well as by embedding unfixed fragments in polyacrylamide or agarose gels. Thus, in these immbolizing preparations the chromophore can photocycle without rotating inside a bacteriorhodopsin monomer by more than our detection limit of 2°–5°. The large rotations we observed in aqueous suspensions of purple membranes were probably due to rotations of entire protein monomers. The process by which a photocycling monomer causes its noncycling neighbors to rotate may help explain the highly cooperative behavior bacteriorhodopsin exhibits when it is aggregated into crystalline arrays of trimers.

INTRODUCTION

The purple membrane can be considered to be a two-dimensional crystal of bacteriorhodopsin trimers arranged in a hexagonal lattice (1–3). Bacteriorhodopsin consists of a chromophore (all-*trans* retinal) covalently linked to the interior of a 26,000 mol wt protein (4). During the photocycle any rotation of the highly dichroic chromophore can be detected using linearly polarized light. In this investigation we photoselected chromophores with a brief actinic flash of linearly polarized light and monitored the resulting dichroism with a measuring light polarized parallel or perpendicular to the photoselecting flash. Both the actinic and measuring wavelengths were in the visible light region, hence the dichroism we observed resulted only from the photoselection and rotations of retinal rather than any of the numerous UV absorbing chromophores within the protein.

Even after a decade of research, the question of whether or not bacteriorhodopsin chromophores rotate within the membrane remains controversial, partly because some of the methods used to immobilize the membrane fragments can also immobilize the proteins within the membrane. Also, most published experiments have not adequately distinguished between the three different types of chromophore rotations that can be detected in dichroism experiments; (*a*) rotations of the entire membrane fragments, (*b*) rotations of the bacteriorhodopsin monomers within the membrane, and (*c*) rotations of the chromophore within monomers of bacteriorhodopsin. Because all three of these rotational motions can occur on the same time scale, we took considerable care to identify and distinguish between them. To date, most observations of photo-induced dichroism have not revealed detectable rotations within the membrane during the lifetime of the photocyle (5, 6, and Poo and Cone, unpublished results). However, both the anisotropies and signal-to-noise ratios of these earlier measurements were low, and, more importantly, the measurements were usually made only at room temperature, a temperature at which we now find the chromophore rotations within the membrane most difficult to detect. Lozier and Niederberger did observe small anisotropy decays during the early stages of photocyle (7) similar to the small decays observed by D. R. O'Brien and R. A. Cone (see Methods). They later attributed this decay to diffusion of small fragments (8). Cherry et al. (9) observed no detectable change in the photo-induced dichroism of cell envelops that contained purple membranes, but the anisotropy was low, <0.2. Only Sherman and Caplan (10) have suggested that intramembrane chromophore rotations occur during the photocycle. They noticed that the temperature dependence of the decay of the photo-induced dichroism in aqueous suspensions of purple membrane fragments was much greater than expected for rotational diffusion of the fragments in water. Our observations agree with those of Sherman and Caplan. Moreover, we find that photo-induced dichroism depends strongly on the measuring wavelength. For example, during the photocycle, the dichroism rises at some wavelengths while simultaneously falling at others. The dichroism can also rise to values that

Dr. Ahl's present address is the Physics Department, Boston University, Boston, MA.

greatly exceed the theoretical maximum attainable by photoselection of a single population of chromophores. These and other observations we report here lead us to conclude that light initiates large rotations not only in the photocycling monomer but also in the noncycling monomers, most likely the two nearest neighbors in each trimer.

Why does bacteriorhodopsin aggregate into trimers? At present, the physiological function of the trimer is unclear. Recently, however, Korenstein et al. found evidence for cooperativity in the photocycle of purple membranes (11). They observed a dependence of the photocycle kinetics on the amount of M intermediate present after steady state illumination conditions. They also noted that cooperativity can be eliminated by disrupting the protein lattice with ether. Moreover, the binding of retinal to apomembrane is highly cooperative with a Hill coefficient of 3 (12) and the bleaching of bacteriorhodopsin with hydroxylamine appears to be highly cooperative (13). We believe that the light-activated protein rotations we report here may underlie these cooperative interactions between protein monomers in the purple membrane.

MATERIALS AND METHODS

Halobacteria halobium strain S_9, was kindly provided by Dr. Walther Stoeckenius. Isolated purple membranes were prepared by osmotic lysis and sucrose gradient centrifugation as described by Becher and Cassim (14). The membrane fragments were stored at a concentration of ~1 mg protein/ml in 10 mM potassium phosphate buffer at pH 7 in the presence of 5 mM sodium azide. This procedure was used to retard bacterial degradation of the fragments. Purple membrane fragments stored without azide often had a small artifactual decay of dichroism during the early photocycle that might be produced by bacterial action. This dichroism was similar to transient dichroism changes first observed by D. R. O'Brien and R. A. Cone (unpublished results). Bacteriorhodopsin concentrations were determined at 570 nm after correcting for light scattering with a Cary 17 spectrophotometer (Cary Instruments, Monrovia, CA) using an extinction coefficient of $6.3 \times 10^4\ M^{-1}\ cm^{-1}$, and a molecular weight of 26,000 g/mol.

In many experiments, the fragments were simply suspended in buffer, since we were concerned that procedures used to immobilize the fragments, such as immobilization in gels, might produce artifacts. We found that at warm temperatures, i.e., over 30°C, the intramembrane chromophore rotations were relatively fast and were not noticeably distorted by fragment rotation. However, at cold temperatures, i.e., ~0°C, the intramembrane rotations were much slower and were on the same time scale as fragment rotations. To distinguish between these two types of chromophore rotations we raised the viscosity of the solution by adding Ficoll 400 (Pharmacia Fine Chemicals, Pharmacia, Inc., Piscataway, NJ) a highly branched, high-molecular-weight polysaccharide. This procedure, as will be discussed later, effectively immobilized the fragments during the period of observation without qualitatively changing, the photo-induced dichroism we observed in buffer. We also investigated the effects of immobilizing the fragments with gels. We mainly used a modification of the procedures of Mowery et al. (15) to immobilize the fragments by mixing them with 7.5% acrylamide, and 0.2% bisacrylamide in degassed water. The gelation was started with 0.3% tetramethylethylenediamine and 0.03% ammonium persulfate. We also used agarose gels prepared by mixing the fragments with 1.5% (wt/vol) agarose. Gelation was started by heating the mixture to 60°C.

Dark-adapted purple membrane fragments were fixed with glutaraldehyde by mixing 1 ml of 8% glutaraldehyde (Polysciences, Inc., Warrington, PA) with 1 ml of dark-adapted purple membrane suspension (1.6 mg protein/ml, in 100 mM borate buffer at pH 9.75) in the dark at room temperature. The reaction was stopped after 1 h by centrifugation and washing. The cross-linking effects of glutaraldehyde fixation were assayed by SDS polyacrylamide gel electrophoresis. The samples were run on 10% gels using the procedures of Laemmi (16) and destained according to the procedure of Fairbanks et al. (17).

The basic design of the micro-flashphotometer is described in reference 18. The actinic flash energy was adjusted to activate ~10% of the bacteriorhodopsin molecules. This flash energy was selected because it gave good signal-to-noise ratios while only slightly reducing the anisotropy. The polarization of successive actinic flashes was alternated exactly 90°, as detected at the sample. The measuring light wavelength was selected by placing different interference filters directly in front of the photomultipliers. This insured that reliable comparisons could be made between results obtained at different wavelengths since the light incident on the sample was not altered in any way when different measuring lights were selected.

The photo-induced dichroism was expressed as the anisotropy, r:

$$r = \frac{\Delta A_{\parallel} - \Delta A_{\perp}}{\Delta A_{\parallel} + 2\Delta A_{\perp}}.$$

Usually we observed photo-induced dichroism at the three measuring wavelengths, on the same sample under identical conditions. The anisotropies could thus be calculated at the same time points in the photocycle for each measuring wavelength. To calculate the anisotropies of the depleted, r_d, and photocycling, r_p, chromophores, the total absorbance change ΔA_T and the depletion absorbance change A_d are needed at two different measuring wavelengths. ΔA_T was determined directly from the records. The depletion absorbance change, which results from the depletion of unactivated chromophores by the actinic flash, could be most accurately determined at 570 nm, since during the M phase of the photocycle the cycling chromophores have little or no absorption at this wavelength. The absorption spectrum of bacteriorhodopsin was then used to calculate the depletion absorbance changes expected at the other two measuring wavelengths. The depletion absorbance change A_d at 570 nm was determined using

$$A_d = \frac{A_0}{1 - \beta}$$

where A_0 is the maximum 570 nm absorbance decrease in the sample determined by extrapolating back to zero time. β is defined as the ratio of the extinction coefficient of the photocycling intermediates present during the maximum decrease in absorbance at 570 nm, divided by the extinction coefficient of bacteriorhodopsin. The photoproduct absorption spectra of Lozier et al. (19) indicate that β is ~0.1. The calculated anisotropies and displacement angles do not show a strong dependence of β and our results are basically the same for all β values ranging from 0.001 to 0.2. The depletion absorbance change at 400 nm was determined using the 400 to 570 nm absorption ratio of bacteriorhodopsin. This ratio, which we call γ, had a value of 0.22 as determined from the absorption spectra of light adapted bacteriorhodopsin. r_d and r_p were calculated in a microcomputer using the following equations:

$$r_d = \frac{r_{570}\left\{\left(\frac{1-\beta}{A_0}\right) - \frac{\gamma}{\Delta A_{400}}\right\} - r_{400}\left\{\left(\frac{1-\beta}{A_0}\right) - \frac{1}{\Delta A_{570}}\right\}}{\frac{1}{\Delta A_{570}} - \frac{\gamma}{\Delta A_{400}}}$$

$$r_p = \frac{\frac{r_{570}\gamma}{\Delta A_{400}} - \frac{r_{400}}{\Delta A_{570}}}{\frac{\gamma}{\Delta A_{400}} - \frac{1}{\Delta A_{570}}}$$

r_{570}, ΔA_{570}, and r_{400}, ΔA_{400} are the observed anisotropies and absorbance changes at 570 and 400 nm.

RESULTS

Evidence for Intramembrane Chromophore Rotation

We found that the rate and temperature dependence of the photo-induced dichroism decay at 570 nm was not consistent with rotational diffusion of purple membrane fragments in buffer. The Q_{10} was ~2.6 for the 570 nm anistropy decay. In addition glutaraldehyde fixation had a dramatic effect, reducing the Q_{10} to ~1.3 which is consistent with rotational diffusion in water. We determined the size of the fragments by electron microscopy. Using Perrin's equations (20) for thin disks we found good agreement between the predicted and observed decay rates for glutaraldehyde fixed fragments, were as the decay rates for the unfixed fragments were significantly faster than predicted.

Perhaps the most convincing evidence that chromophore rotations occur within the purple membrane comes from observations of dichroism at different measuring wavelengths. Fig. 1 *a* shows records obtained at three different wavelengths from unfixed fragments in buffer at 30°C, and Fig. 1 *b* shows the resulting anisotropies calculated from these same records. The anisotropy at 570 nm decayed rapidly at this temperature but the anisotropy at 400 nm increased. We have observed this behavior consistently in dozens of experiments, and we have been unable to think of any mechanism by which rotational motion of fragments could yield such records.

The photo-induced dichroism varied strongly with both temperature and wavelength. At temperatures near 0°C, the anisotropy at 570 nm decayed more slowly, as expected from the Q_{10}, however, the anisotropy at 400 nm decayed significantly faster than the 570 nm anisotropy. At this cold temperature the anisotropy decays were somewhat distorted by the rotational diffusion of the fragments. To slow fragment rotations as gently as possible, we added Ficoll to the buffer. This multibranched, high-molecular-weight polysaccharide markedly raises the viscosity of the solution, but does not form rigid gels. Also, it does not significantly partition into membranes nor raise the osmotic pressure. As shown in Fig. 2 *b*, 30% Ficoll raised the viscosity enough to essentially stop fragment rotation on this time scale, since the anisotropy at 570 nm rose slightly at first and then became constant. The 400 nm anisotropy decayed, though somewhat more slowly than without Ficoll, and the 650 nm anisotropy rose dramatically, rising significantly beyond 0.4, the theoretical maximum anisotropy that can be induced in a single population of chromophores by a photoselecting actinic flash. This unusual result is readily apparent in the 650 nm record shown in Fig. 2 *a*. The perpendicular recording rose above the basline while the parallel recording remained below. Again, we have been unable to explain such an unusual result on the basis of fragment rotations. Ficoll had no significant effect on the anisotropies observed in warm temperature experiments. The only obvious effect of Ficoll

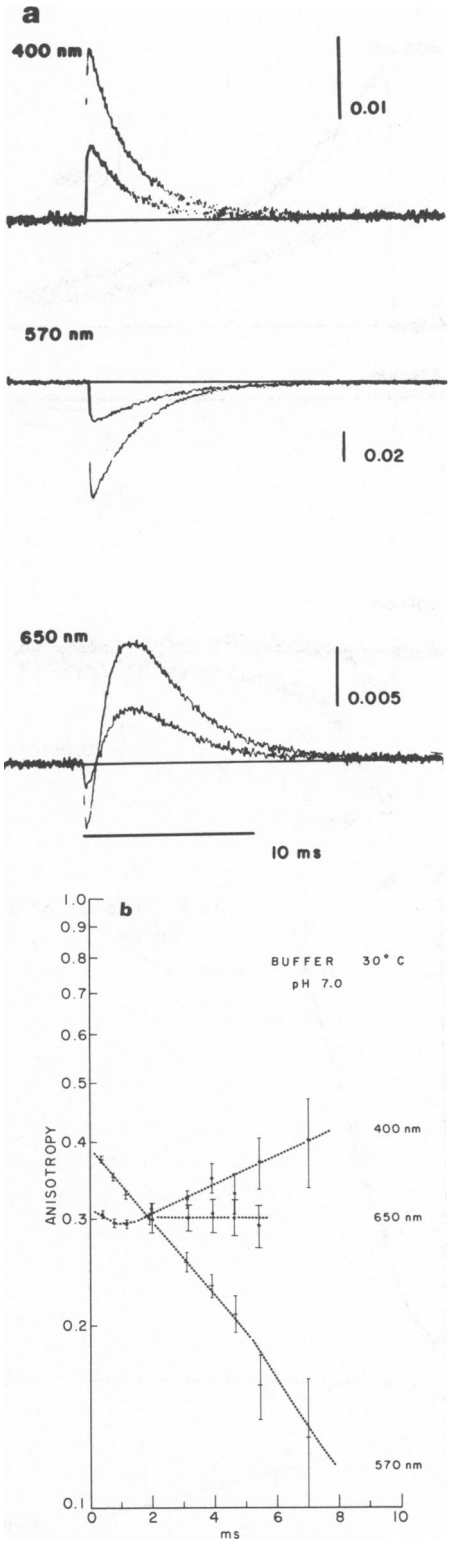

FIGURE 1 (*a*) Absorbance changes observed at three different measuring wavelengths for purple membranes suspended in buffer. Parallel and perpendicular records were obtained by alternately irradiating the sample with an actinic flash polarized parallel or perpendicular to the effective polarization of the measuring light (30°C, 10 mM phosphate buffer, pH 7.0). (*b*) The anisotropies of the absorbance changes shown in Fig. 1 *a* plotted as a function of time after the actinic flash. The error bars show the 68% confidence limit set by the noise level of the recordings.

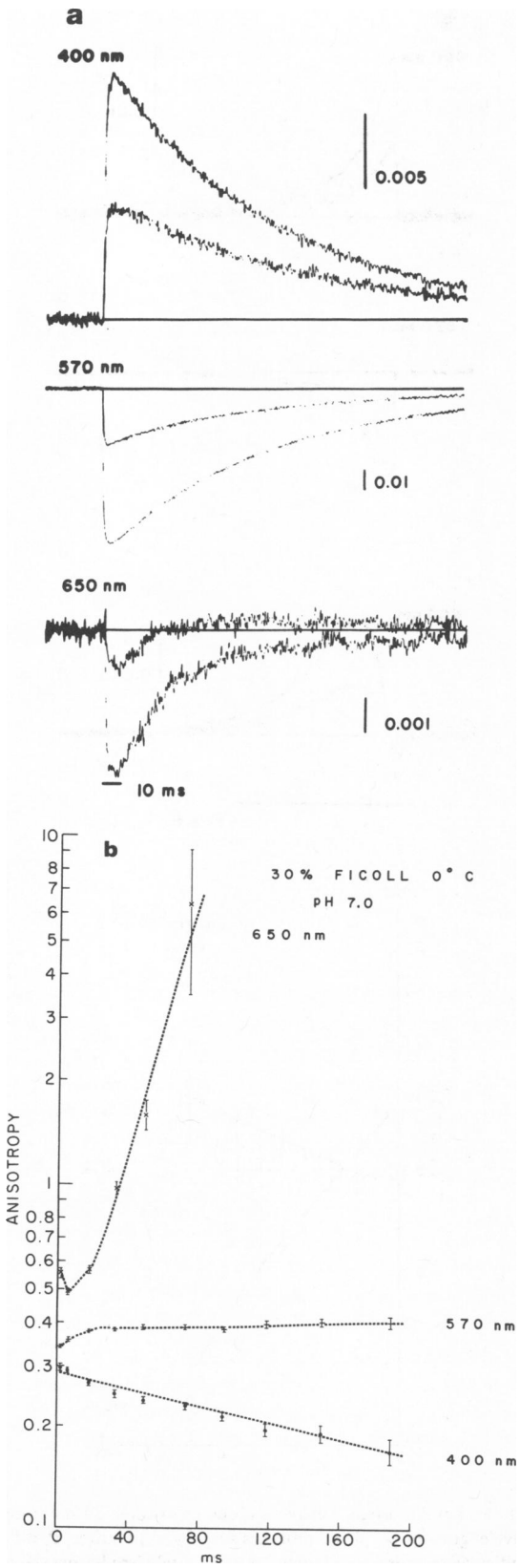

FIGURE 2 (*a*) Absorbance changes from purple membranes suspended in 30% (wt/vol) Ficoll at 0° (10 mM phosphate buffer, pH 7.0). (*b*) The anisotropies for the records shown in Fig. 2 *a*. Note that the 650 nm anisotropy rises rapidly and greatly exceeds 0.4.

was to somewhat slow the rates of the decay in anisotropy at 570 nm.

We also examined the effect of pH. Over a pH range of 5 to 9 there were no striking changes in the photo-induced dichroism. However, alkaline pH's of 9 or above markedly slowed the photocycle. Hence, we could observe the anisotropy changes for longer time intervals. Typical warm temperature alkaline records are shown in Fig. 3. Ficoll was added to slow fragment rotational diffusion. These records clearly indicate that a 570 nm dichroism decay occurs simultaneously with a 400 nm dichorism increase.

Glutaraldehyde fixation with our procedures extensively cross-linked bacteriorhodopsin beyond trimers as determined by SDS gel electrophoresis. Thus, if the wavelength dependence of the dichroism was produced by protein rotations glutaraldehyde fixation should eliminate it. However, since glutaraldehyde fixation left the fragments free to rotate, this procedure should not disturb any changes in anisotropy produced by fragment rotations. Glutaraldehyde fixation entirely eliminated the diverging anisotropies at 400 and 570 nm at both warm and cold temperatures. After fixation the anisotropies were the same at both wavelengths and both anisotropies decayed at the same rate. The decay rates were consistent with the measured viscosity of the Ficoll solutions and the size of the fragments. Near 0°C in 30% Ficoll the glutaraldehyde fixed chromophores did not rotate during the measurement

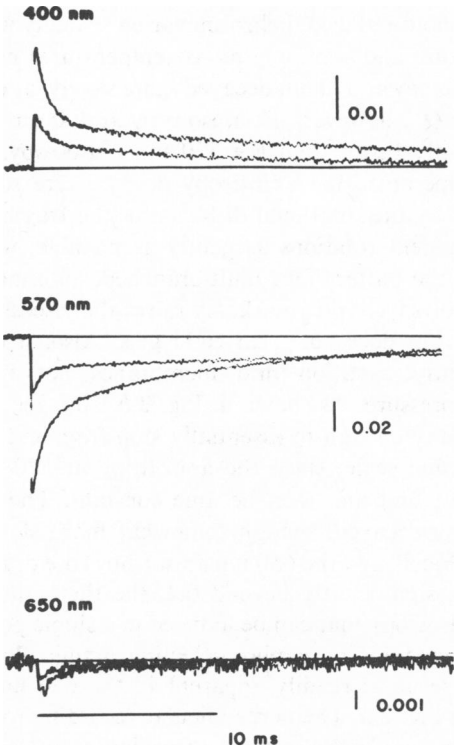

FIGURE 3 (*a*) Absorbance changes from purple membranes suspended in 30% (wt/vol) Ficoll (35°C) using 50 mM borate buffer to achieve a pH of 9.25. Note the marked anisotropy decay at 570 nm, and the crossing of the recording well below the baseline.

period as shown by Fig. 4. Like glutaraldehyde, formaldehyde reacts with free amino groups (21), but fixation with 400 mM formaldehyde did not cross-link bacteriorhodopsin and did not eliminate the unusual wavelength dependence of the photo-induced dichroism. These fixation experiments suggest that the chromophore rotations probably result from protein (monomer) rotations rather than chromophore rotations within the protein. However, glutaraldehyde fixation dramatically slowed the photocycle raising the possibility that it might also be altering or reducing intraprotein chromophore rotations as well.

It has been reported that immobilizing purple membrane fragments in agar gels at 18°C totally eliminates any time dependence of photo-induced dichroism (22). We find, in agreement with these results, that both 7.5% polyacryamide and 1.5% agarose gels can eliminate the decay of anisotropy at 570 nm, particularly at room temperatures, as shown in Fig. 5. However, at warmer temperatures, (i.e., above 30°C) we did observe anisotropy decays and rises in 7.5% polyacryamide similar to those we obtained with the fragments in buffer. We are not sure of the mechanism by which these gels immobilize the rotations at colder temperature, but it is important to note that even very dilute gels, such as 1.5% agarose, could significantly affect the interactions between bacteriorhodopsin monomers since the spacing of the meshwork in even this dilute a gel is comparable with the spacing between trimers (23). Unlike glutaraldehyde fixation, chromophore immobilization observed in gels did not noticeably alter the photocycle which indicates very little if any chromophore rotation within the protein (see Discussion section).

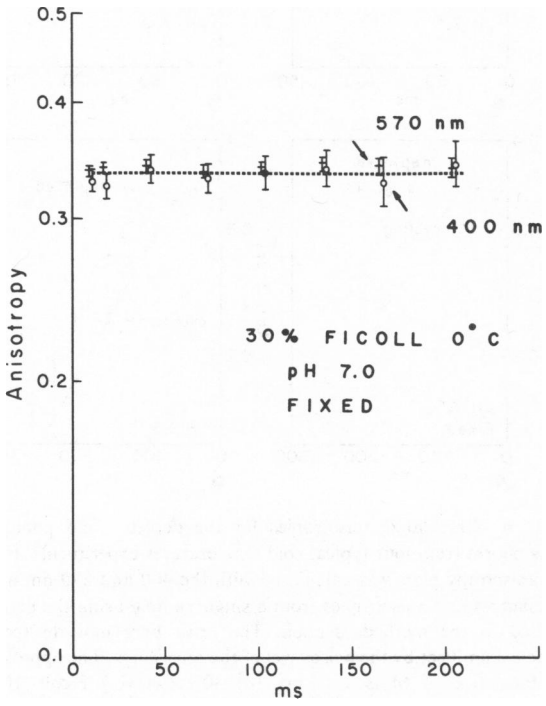

FIGURE 4 Anisotropy changes from a suspension of glutaraldehyde fixed purple membrane fragments in 30% (wt/vol) Ficoll at 0°C (10 mM phosphate buffer pH 7.0).

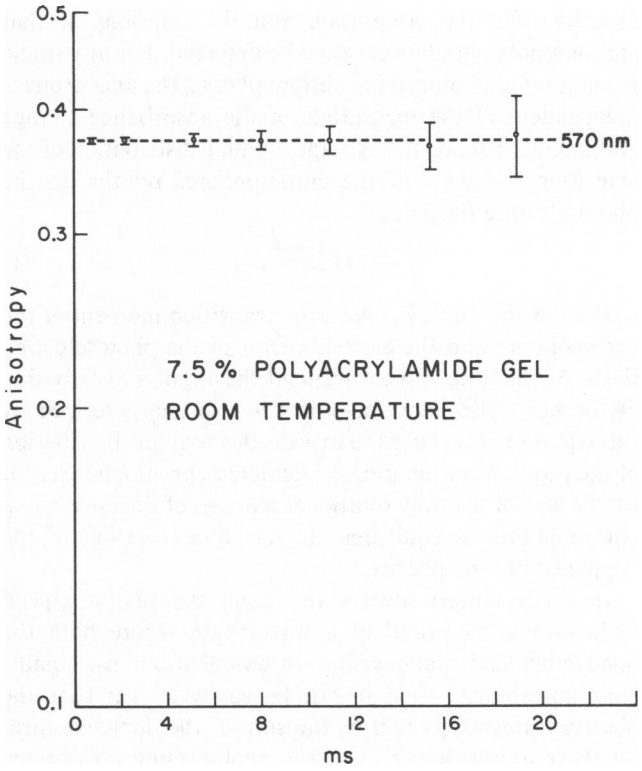

FIGURE 5 Anisotropy changes at 570 nm from purple membrane fragments immobilized in 7.5% polyacryamide gels at room temperature.

Two Population Analysis

Theories for photoselection and rotational diffusion have been developed to analyze the rotational motions of fluorophores (24), and more recently chromophores (25), but these analyses cannot account for the unusual photo-induced dichroism we report here. Thus our results led us to extend existing photoselection theory[1] (18). In particular, we have extended the theory to account for independent rotations in two different chromophore populations, the photoactivated and the unactivated chromophores.

The actinic flash not only produces an oriented population of photoactivated chromophores, it also eliminates an oriented population of unactivated chromophores. The polarized measuring light thus measures the sum of the absorbance decrease due to the depletion of unactivated chromophores and the absorbance increase due to the formation of photoproduct chromophores. In the case of bacteriorhodopsin, we will designate all the photoproduct chromophores as the "photocycling," and all the unactivated chromophores as the "noncycling" chromophores.

If the photo-induced dichroism could be measured at a wavelength where only one chromophore population

[1]A similar analysis was independently developed by Czégé et al. (22).

absorbs, only the orientation and the rotations of that chromophore population would be detected. For any single population of photocycling chromophores, the anisotropy is independent of the magnitude of the absorbance change and directly reveals the average angular distribution of the transition moments of the chromophores relative to the photoselecting flash (18):

$$r = \tfrac{1}{2}\{3\,\overline{\cos^2\theta} - 1\} \quad (1)$$

where θ is the angle between the transition moment of the chromophore and the electric vector of the photoselecting flash. At the time of measurement the angular distribution of the noncycling chromophores is also characterized by this equation if it is used to express the angular distribution of the positions of imaginary "depleted chromophores." It can be shown that any rotational motions of the noncycling chromophores is equivalent to an equal rotation of the "depleted chromophores."

If, as is almost always the case, the photo-induced dichroism is measured at a wavelength where both the noncycling and photocycling chromophores have significant absorbance, then it can be easily shown that the observed anisotropy will be the sum of the depleted chromophore anisotropy, r_d, and the photocycling anisotropy, r_p, weighted by their share of the total absorbance change:

$$r = \frac{A_d}{\Delta A_T} r_d + \frac{A_p}{\Delta A_T} r_p \quad (2)$$

where

$$\Delta A_T = A_d + A_p.$$

ΔA_T is the total absorbance change at time, t, after the flash. A_d is absorbance decrease due to depletion of the noncycling chromophores. This absorbance change will always be negative. A_p is the absorbance increase at time t, due to the formation of photocycling chromophores.

Because both A_d and A_p will depend on the wavelength of the measuring light, it is clear that r will be a function of wavelength. Only when the depleted chromophores and the photocycling chromophores both have the same anisotropy will the observed anisotropy be independent of the measuring wavelength. Thus, the photo-induced anisotropy will be independent of measuring wavelength whenever both the unactivated and photoproduct chromophores undergo the same rotations, such as when a membrane fragment rotates. However, when the photo-induced anisotropy is wavelength dependent, two or more chromophore populations must undergo different rotations. In this case, Eq. 2 can be used to calculate the anisotropies of the depleted and the photocycling chromophores. If the anisotropy and absorbance change are measured at two different wavelengths in the same preparation at the same time point in the photocycle, these values can be inserted into Eq. 2 to give two simultaneous equations that can be solved for both r_d and r_p. Thus, anisotropies and absorbance changes recorded at two measuring wavelengths can be transformed into the anisotropies of two chromophore populations: the depleted and the photocycling chromophores.

Results of the Two-Population Analysis

We calculated r_d and r_p as a function of time using the 570 nm dichroism in combination with either the 400 nm data or the 650 nm data. Because the 570 and 400 nm records usually had the best signal-to-noise ratios, they provided more precise results, and the calculated anisotropies shown in this section used this pair of wavelengths. However, it is important to note that calculations using the 570 and 650 nm data indicated similar chromophore rotations.

The calculated anisotropies of the two chromophore populations are shown for four typical cold temperature experiments in Fig. 6. At the earliest analyzable time point after the actinic flash the anisotropy of the photocycling chromophores was lower than the anisotropy of the depleted chromophores. Hence, at this early stage of the cycle, the photocycling chromophores were more rotationally displaced than their noncycling neighbors. During the

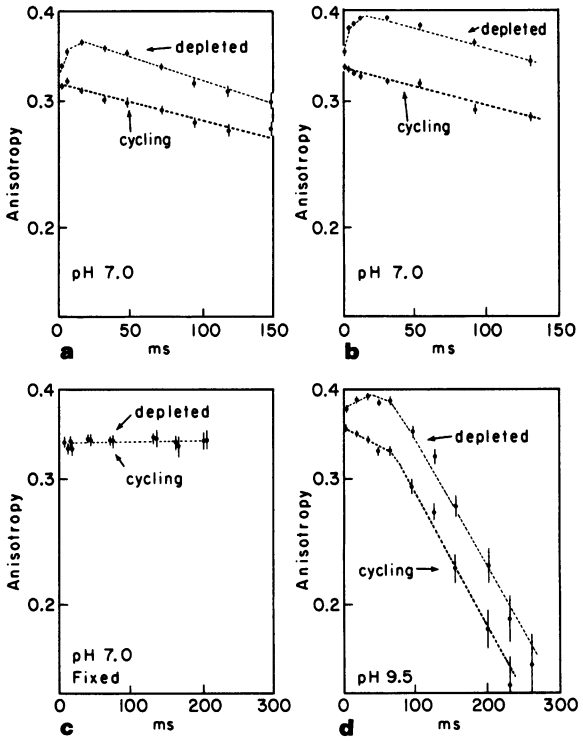

FIGURE 6 Calculated anisotropies for the depleted and photocyling chromophores from four typical cold temperatures experiments. Each of these anisotropy plots was calculated with the 400 and 570 nm absorbance changes and anisotropies from a single sample using the equations discussed in the methods section. The error bars indicate the 68% confidence limit set by the noise level of the recordings. The approximate peak formation of M is at 5 ms. (*a*) 30% (wt/vol) Ficoll, 10 mM phosphate buffer, pH 7.0, 0°C; (*b*) 30% (wt/vol) Ficoll, 10 mM phosphate buffer, pH 7.0, 2°C; (*c*) glutaraldehyde fixed, 30% (wt/vol) Ficoll, 10 mM phosphate buffer, pH 7.0, 0°C; (*d*) 30% (wt/vol) Ficoll, 50 mM borate buffer, pH 9.25, 3°C.

formation of the M intermediate the anisotropy of the depleted chromophores increased, indicating that these noncycling chromophores were reorienting themselves toward their initial angular distribution. In contrast, the photocycling chromophores did not reorient during this period. After the peak formation of M both populations of chromophores commenced a slow, prolonged decay in anisotropy. This "parallel" decay in anisotropy indicates that similar rotational disordering must have occurred simultaneously in both the noncycling and photocycling chromophore populations. Glutaraldehyde fixation eliminated all these rotations in both populations, as shown in Fig. 6 *c*.

It is difficult to estimate how far each population rotated from the initial orientation because our calculations are limited by the time resolution of the measurements. However, photoselection theory predicts that the initial anisotropy of each chromophore population can at most approach, and never exceed, 0.4 (26, 27). Moreover, neither chromophore population can subsequently attain an anisotropy that exceeds the initial anisotropy produced by the photoselecting flash. Thus, in Fig. 6, the initial chromophore anisotropies must be at least as large as the anisotropy of the depleted chromophores observed near the peak formation of M at ~5 ms. This indicates that both chromophore populations must have rapidly disoriented prior to the first analyzable time point. We have some direct, unpublished evidence for this initial disorientation process. Using a krypton laser to increase the time resolution, we observed at cold temperatures that the anisotropy at 570 nm first decreases and then increases during the decay of K and L intermediates. The magnitude of the initial disordering event can be calculated from the results shown in Fig. 6 using Eq. 3 (28). The average isotropic angular displacement is given by

$$\Delta\theta = \arccos\sqrt{\frac{\frac{3r_t}{r_i}+1}{3}} \qquad (3)$$

where r_i is the initial anisotropy created by the actinic flash prior to any chromophore rotations and r_t is the anisotropy at time t. By comparing the maximum anisotropy of the depleted chromophores (which averaged 0.37 ± 0.03 at cold temperatures) with the largest photocycling anisotropy, we calculate that both populations must have undergone an initial disordering displacement of ~15°–20°.

Following this initial disordering rotation, at cold temperatures, the noncycling chromophores returned toward their original orientations. Clearly such reordering cannot be due to rotational diffusion of bacteriorhodopsin molecules. It must instead involve interactions with the protein lattice to provide the reference directions needed for reordering these noncycling chromophores. The photocycling chromophores did not reorient during this process and thus remained displaced relative to their noncycling neighbors. The average isotropic angular displacement of the photocycling chromophores relative to depleted chromophores calculated to be ~17°–20°. As the photocycle continued, displacement between the two chromophore populations remained essentially constant even though both populations commenced a slow but extensive rotational disordering process, as shown in Fig. 6 *d*. The average relaxation time for this slow rotation was 0.66 ± 0.32 s when the fragments were suspended in 30% Ficoll. This rotation, though slow, was not due to fragment rotation, since the rotations of glutahaldehyde fixed fragments in Ficoll were undetectable over this time interval (Fig. 6 *c*).

The calculated anisotropies, r_d and r_p, for four typical warm temperature experiments are shown in Fig. 7. Again, at the earliest time point after the actinic flash the photocycling chromophores were more rotationally displaced than their noncycling neighbors. (The earliest measured anisotropy of the depleted chromophores for temperatures over 30°C was 0.35 ± 0.02.) However, the early rise in anisotropy of the depleted chromophores, which was easily observed at cold temperatures, was not detected at

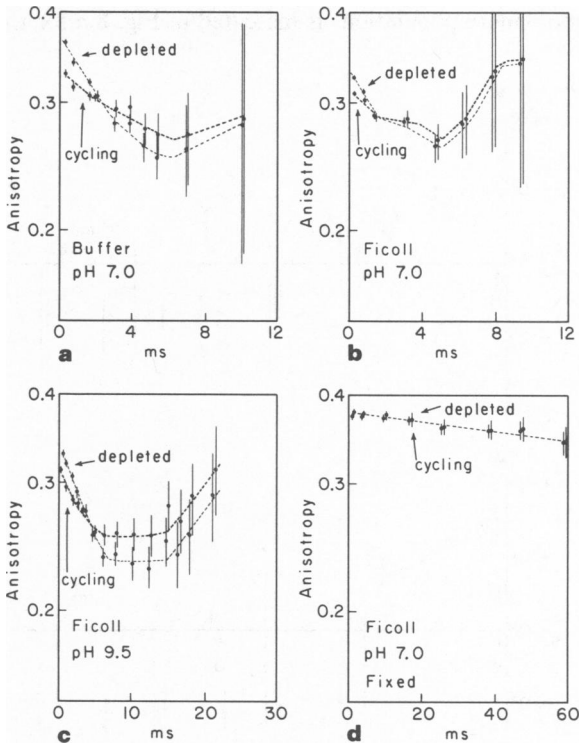

FIGURE 7 Calculated anisotropy for the depleted and photoproduct chromophores from four typical warm temperature experiments. Each of these anisotropies was calculated with the 400 and 570 nm absorbance changes and anisotropies from a single sample using the equations discussed in the methods section. The error bars indicate the 68% confidence limit set by the noise level of the recordings. (*a*) 10 mM phosphate buffer, pH 7.0, 30°C; (*b*) 30% (wt/vol) Ficoll, 10 mM phosphate buffer, pH 7.0, 30°C; (*c*) 30% (wt/vol) Ficoll, 50 mM borate buffer, pH 9.5, 35°C; (*d*) glutaraldehyde fixed, 30% (wt/vol) Ficoll, 10 mM phosphate buffer, pH 7.0, 35°C.

warm temperatures, possibly because this early reordering process was too fast to be detected by our equipment. Also, at warm temperatures the depleted chromophore anisotropy decayed more rapidly than the photoproduct anisotropy. This indicates that the photocycling chromophores disordered more slowly during this phase of the cycle than did their neighbors until eventually the photocycling chromophores became more oriented than the noncycling chromophores. Late in the cycle, as shown in Fig. 7, the anisotropy of both chromophore populations appears to plateau, and perhaps even increase. Thus, the major "parallel" disordering process detected at cold temperatures did not appear at warm temperatures. Glutaraldehyde fixation, as shown in Fig. 7 *d*, again eliminated all detectable chromophore rotations other than fragment rotations.

The error bars shown in Fig. 7 are quite large near the end of the photocycle because the absorbance changes eventually become quite small. However, these error bars show only the overall uncertainty of the absolute anisotropy of the chromophore populations, they do not indicate the much smaller uncertainty of the differences between the two chromophore populations, as can be seen in Fig. 8. The angular displacement difference between the two chromophore populations is indicated in Fig. 8 *a* for three

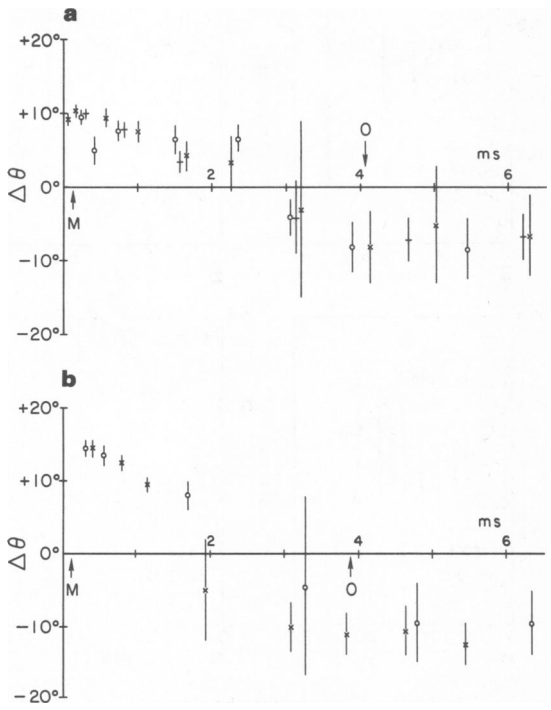

FIGURE 8 Angular displacement differences ($\Delta\theta$) between the photocycling and noncycling chromophores for several warm temperature experiments. Positive angular displacement differences indicate the photocycling chromophores were more rotationally displaced than noncycling chromophores. The approximate peak formation of M and O are indicated by the arrows. (*a*) Three experiments using fragments suspended in 30% (wt/vol) Ficoll at 30°C (0), 32°C (×), and 32°C (+) (10 mM phosphate buffer, pH 7.0). (*b*) Two experiments using fragments suspended in 10 mM phosphate buffer, pH 7.0, at 30°C (×) and 31°C (0).

experiments with purple membranes suspended in 30% Ficoll and in Fig. 8 *b* for two buffer experiments. The arrows indicate the approximate times of the peak formation of the M and O intermediates. Positive angles indicate the photocycling chromophores are more displaced, while negative angles indicate the noncycling chromophores are more displaced. These figures show that prior to the first observed time point the photocycling chromophores became ~10° more displaced than the noncycling chromophores. However, as the cycle progressed to the peak formation of 0, the photocycling chromophores became relatively less disordered than their noncycling neighbors by 5–10°. It appears from Fig. 7 that the photocycling molecules lead the way back toward the initial orientation.

DISCUSSION

It seems likely that any chromophore rotation during the photocycle may provide some clue about the proton pumping mechanism, and several investigators have used polarized light to try to detect such rotations. Most have concluded that no significant rotations occur within the membrane (5, 6, and Poo and Cone, unpublished results). However, our observations compel us to conclude that intramembrane chromophore rotations do in fact occur. Close comparison of results from different investigations is difficult since experimental conditions and procedures have varied, and many conditions such as temperature, measuring wavelength, and suspending medium all influence the observed dichroism. Most important, we find that the dependence of dichroism on measuring wavelength is especially weak at room temperatures, where most earlier observations have been made.

The observation least consistent with ours was recently reported by Kouyama et al. (29) who measured, at 25°C, the transient dichroism produced at 550 nm in purple membrane suspensions both by photoselection and by electric fields. They observed the same anisotropy decay rate with both techniques, suggesting that under their conditions all chromophore rotations within the membrane were small compared with fragment rotations. Unfortunately, they reported photo-induced dichroism at only one temperture and one measuring wavelength, and hence would not have detected temperature and wavelength differences that might have revealed intramembrane chromophore rotations.

Our results confirm earlier work that has demonstrated that the chromophore can proceed through the photocycle, in some preparations, without detectable rotations. We found that fixing the fragments with glutaraldehyde effectively eliminated chromophore rotations, but this procedure also greatly slowed the photocycle and apparently eliminated the 0 intermediate (Ahl and Cone, unpublished results). Thus, we think it is especially significant that dilute gels such as agarose or polyacrylamide can apparently eliminate all detectable rotations, at least at room

temperature, without noticeably altering the photocycle. Czégé et al. (22) have recently shown that even in a 1% agar gel they could not detect chromophore rotations. Because such gels have average meshwork spacings comparable with the spacing between bacteriorhodopsin trimers and because any tendency of the gel to adsorb to the membrane could produce even smaller meshwork spacings, it is reasonable to suppose that gels could immobilize the rotations of trimers and possibly large monomer rotations within the trimer. However, it seems highly unlikely that gels can immobilize chromophore rotations within the protein while not altering the photocycle. Thus, we believe the gel results provide the best available evidence that during the photocycle the chromophore undergoes little or no rotational motion within the protein. (It is important to remember that although we have observed chromophore immobilization in gels near room temperatures, at slightly higher temperatures we have observed wavelength-dependent dichroism decays and rises indicating intramembrane chromophore rotations [data not shown].)

Because both gels and glutaraldehyde fixation indicate that the chromophore is immobilized within the photocycling monomer, the large intramembrane chromophore rotations we observed in aqueous suspensions are almost certainly caused by large rotations of the protein monomers. An independent line of reasoning leads to a similar conclusion. Because the photocycling monomers cause the chromophores in their noncycling neighbors to rotate by some 10–15° it is difficult to conceive how such large rotations could occur in the noncycling chromophores unless the entire noncycling monomer rotates, given the structure and spacing of bacteriorhodopsin molecules within the trimer and the probable location of the chromophore within each monomer (30, 31).

We do not know the axes of the chromophore rotations, since our experiments were done with randomly oriented fragments. However, if all the rotations result from protein rotations, then they probably all occur about an axis normal to the plane of the membrane, since bacteriorhodopsin does not appear to "tumble" in the membrane (32). Also, dichroism experiments with oriented multilayer films of bacteriorhodopsin showed no change in the "tilt" of the chromophore in the plane of the membrane, i.e., no out-of-plane rotation occurred in forming the M intermediate (33).

Because the photocycling monomers undergo different rotations than their noncycling neighbors, at least some of the rotations are certainly due to the action of light. But, are all the rotations we observed initiated by light or do some continuously occur in the dark? Kornenstein and Hess (34) measured the dichroism of dark adaptation in thin, hydrated layers of purple membranes at 40°C and detected no change in the anisotropy over a period of 30 min, suggesting that no chromophore rotations occurred during this time. Similarly, none of our data requires or even suggests that any chromophore rotations occur in the dark. Instead, some of our observations at both the warm and cold temperatures, particularly at high pH, suggest that all the rotations we observed are initiated by light. For example, in the warm-temperature experiment analyzed in Fig. 7 *c*, the anisotropy apparently rises as the photocycle ends. More strikingly, at cold temperatures, the anisotropy of the depleted chromophores rises sharply as the M intermediate is forming, as shown in Fig. 6. These results strongly indicate light must have disordered the chromophores, since any increase in dichroism must result from the molecules reorienting after having been disordered by the actinic flash. Finally, in the cold-temperature experiment shown in Fig. 6 *d*, the slow "parallel" decay in anisotropy of the depleted chromophores extrapolates to the theoretical maximum of 0.4 at ~70 ms after the actinic flash. This implies that the noncycling chromophores only began to undergo the slow rotation process some 70 ms after the actinic flash. Thus, this process could not have been occurring continuously in the dark, but must have been initiated by the actinic flash.

Recently, two groups of investigators have discovered light-induced changes in the structure of the purple membrane that may be related to the rotations reported here. Tokutomi et al. (35) have observed a flash-induced transient increase in the membrane fluidity of the purple membrane on a time scale comparable to the photocycle. Frankel and Forsyth (36) have obtained nanosecond-exposure x-ray diffraction patterns from purple membrane that show reversible changes between the diffraction patterns of light stimulated and unstimulated samples.

A summary of the interpretation of our observations is depicted in Fig. 9. In the dark, the trimer is essentially immobile, but within 1 ms after a photon is absorbed by one member of the trimer, both the cycling monomer and its noncycling neighbors undergo 15°–20° rotations (not shown in the figure). After this initial disordering, the noncycling chromophore reorient themselves during the formation of the M intermediate. Thus, in our summary diagram we show the photocycling monomer M, rotated 15° while the noncycling proteins are shown as having returned to their original orientations in the trimer. This disordering-reordering process could only be detected at cold temperatures; at warm temperatures it was probably too rapid for our equipment to detect. During the decay of the M intermediate at physiological temperatures, both the cycling and noncycling chromophores begin a second process of disordering rotations, and during this process the cycling monomers for the first time become more ordered than their noncycling neighbors by ~10° (see Figs. 7 and 8). The upper right corner schematic of Fig. 9 indicates how this could occur. Moreover, toward the end of this process, the anisotropies clearly reach a plateau, and may even rise toward the end of the photocycle (Fig. 7). These results suggest that the cycling monomers begin to reorder first themselves and then their noncycling neighbors towards the end of the cycle.

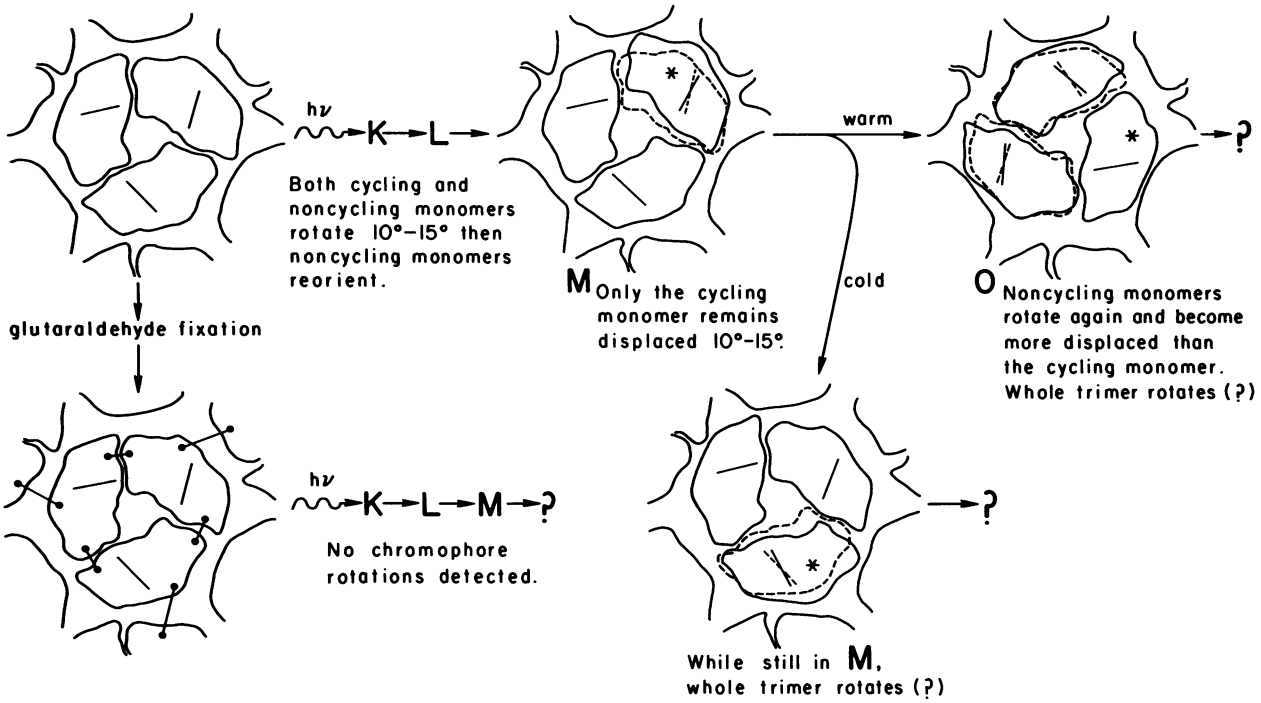

FIGURE 9 Summary figure to illustrate the protein rotations discussed in this paper. The aim of this figure is to give some idea of the magnitudes and sequences of the rotations; obviously, dichroism experiments cannot reveal the details of the actual rotations nor the actual protein-protein relationships. The solid line figures indicate the position of the bacteriorhodopsin monomers in the purple membrane lattice while the short straight lines indicate the orientations of the chromophores. The *upper left*-hand drawing shows the trimer in the dark with the monomers arranged around a threefold symmetry axis. Absorption of a photon by one monomer appears to cause a rapid rotation of all three monomers that is followed by a reorientation of only the noncycling monomers (not shown in the figure). Thus, by the peak formation of the M intermediate, only the cycling monomer remains rotationally displaced some 10°–15°, as shown. The cycling monomer is indicated by an asterisk and its original position in the trimer is indicated by the dashed line (---); its actual position is, of course, unknown. At cold temperatures both the cycling and noncycling chromophores continue to rotate, but the angle between the two chromophore populations does not change. One possible mechanism for this "parallel" decay is rotation of the entire trimer, as shown in the *lower right*-hand figure, which depicts the photoactivated trimer after it has rotated, or "hopped," by 120° to another equivalent "rest" position in the purple membrane lattice. A hopping mechanism for trimer rotation could result in considerable rotational motion of trimers without significant disruption of the membrane lattice, since at any given time only a minute fraction (perhaps <1 in 10^5) of the trimers would be in the process of hopping. This could explain how large protein rotations could be consistent with sharp diffraction patterns. At warm temperatures, after the peak of M, both the cycling and noncycling chromophores begin a second disordering process during which the cycling chromophores for the first time become more ordered than the noncycling chromophores. We have shown one way this might happen in the *upper right*-hand figure by displacing the noncycling monomers in the trimer by 10° and rotating the trimer by ~60°. (This figure thus depicts how a trimer might appear during a hop.) As indicated by the question marks we do not know the chromophore orientations at the end of the photocycle, since the signal-to-noise level falls as the cycle reaches completion. Glutaraldehyde fixation, or embedding the membranes in gels, eliminated all detectable chromophore rotations, but did not eliminate the photocycle.

At cold temperatures the photocycle is greatly slowed, and during the decay of the M intermediate a slow but major disordering process begins that obscures any smaller rotations that might occur within each trimer late in the photocyle. During this major disordering process both the cycling and noncycling chromophores rotate at the same rate (Fig. 6 *d*), and both rotate more than 30°. This suggests that the photocycling monomer by remaining displaced some 15° with respect to its neighbors, frees the trimer from the protein–protein interactions that normally immobilize it in the crystalline lattice, and the whole trimer begins to undergo slow rotational motion as shown in the lower right figure. This slow rotational motion of the trimer may also occur at warm temperatures, but in this case, the photocycle reaches completion before substantial rotational diffusion can occur. Finally, Fig. 9 emphasizes that cross-linking the proteins with glutaraldehyde (or embedding the fragments in gels) can eliminate all detectable chromophore rotations within the purple membrane.

What is the physiological role of these large intratrimer rotations? As we mentioned in the introduction, we believe these rotations may underlie cooperative interactions within the purple membrane. These rotations may even play a role in the proton pumping mechanism. Although we know that monomers pump protons (37) and that membrane fragments immobilized in gels also pump protons (38), we do not yet know how the quantum efficiency of proton pumping changes as the monomers aggregate to form the purple membrane. Perhaps in the purple membrane the cycling monomer elicits help from its neighbors.

We thank Walther Stoeckenius for supplying us with strain S_9 of *Halobacterium halobium*, Mark Dumont for obtaining electron micrographs of fixed and unfixed fragments of purple membrane, and John Nagle for helpful criticism of this work.

This work was supported in part by National Institutes of Health grant EY 520.

Received for publication 4 January 1983 and in final form 22 December 1983.

REFERENCES

1. Henderson, R. 1975. The structure of the purple membrane from *Halobacterium halobium*: analysis of the x-ray diffraction pattern. *J. Mol. Biol.* 93:123–138.
2. Blaurock, A. E. 1975. Bacteriorhodopsin: a trans-membrane pump containing α-helix. *J. Mol. Biol.* 93:139–158.
3. Unwin, P. N. T., and R. Henderson. 1975. Molecular structure determination by electron microscopy of unstained crystalline specimens. *J. Mol. Biol.* 94:425–440.
4. Oesterhelt, D., and W. Stoeckenius. 1971. Rhodopsin-like protein from the purple membrane of *Halobacterium halobium*. *Nature* (*Lond.*). 233:149–152.
5. Naqvi, K. R., J. Gonzalez-Rodriquez, R. J. Cherry, and D. Chapman. 1973. Spectroscopic technique for studying protein rotations in membranes. *Nature* (*Lond.*). 245:249–251.
6. Sherman, W. V., M. A. Slifkin, and S. R. Caplan. 1976. Kinetic studies of phototransients in bacteriorhodopsin. *Biochim. Biophys. Acta.* 423:238–248.
7. Lozier, R. H., and W. Niederberger. 1977. The photochemical cycle of bacteriorhodopsin. *Fed. Proc.* 36:1805–1809.
8. Stoeckenius, W., R. H. Lozier, and R. A. Bogomolni. 1979. Bacteriorhodopsin and the purple membrane of halobacteria. *Biochim. Biophys. Acta.* 505:215–278.
9. Cherry, R. J., M. P. Heyn, and D. Oesterhelt. 1977. Rotational diffusion and exciton coupling of bacteriorhodopsin in the cell membrane of *Halobacterium halobium*. *FEBS* (*Fed. Eur. Biochem. Soc.*). *Lett.* 78:25–30.
10. Sherman, W. V., and S. R. Caplan. 1977. Chromophore mobility in bacteriorhodopsin. *Nature* (*Lond.*). 265:273–274.
11. Korenstein, R., B. Hess, and M. Markus. 1979. Cooperativity in the photocycle of purple membrane of *Halobacterium halobium* with a mechanism of free energy transduction. *FEBS* (*Fed. Eur. Biochem. Soc.*). *Lett.* 102:155–161.
12. Rehorek, M., and M. P. Heyn. 1979. Binding of all-trans retinal to the purple membrane. Evidence for cooperativity and determination of the extinction coefficient. *Biochemistry.* 18:4977–4983.
13. Brecher, B., and J. Y. Cassim. 1977. Effects of breaching and regeneration on the purple membrane structure of *Halobacterium halobium*. *Biophys. J.* 19:285–297.
14. Becher, B. M., and J. Y. Cassim. 1975. Improved isolation procedures for the purple membrane of *Halobacterium halobium*. *Prep. Biochem.* 5:161–178.
15. Mowery, P. C., R. H. Lozier, Q. Chae, Y-W. Tseng, M. Taylor, and W. Stoeckenius. 1979. Effect of acid pH on the absorption spectra and photoreactions of bacteriorhodopsin. *Biochemistry.* 18:4100–4107.
16. Laemmli, U. K. 1970. Clevage of structural proteins during the assembly of the head of bacteriophage T4. *Nature* (*Lond.*). 277:680–685.
17. Fairbanks, G., T. C. Steck, and D. F. H. Wallach. 1971. Electrophoretic analysis of major polypeptides of the human erythrocyte membrane. *Biochemistry.* 10:2606–2616.
18. Ahl, P., and R. Cone. 1982. Photodichroism and rotational motion of rhodopsin and bacteriorhodopsin. *Methods Enzymol.* 88:741–750.
19. Lozier, R. H., R. A. Bogomolni, and W. Stoeckenius. 1975. Bacteriorhodopsin: a light-driven proton pump in *Halobacterium halobium*. *Biophys. J.* 15:955–962.
20. Perrin, F. 1934. Movement brownein d'un ellipsoid (I) dispersion dielectriquie pour des molecules ellipsoidales. *J. Phys. Radium.* 5:497–511.
21. Peters, K., and F. M. Richards. 1977. Chemical cross-linking: reagents and problems in studies of membrane structure. *Annu. Rev. Biochem.* 46:523–551.
22. Czégé, J., A. Dér, L. Zimányi, and L. Keszthelyi. 1982. Restriction of motion of protein side chains during the photocyle of bacteriorhodopsin. *Proc. Natl. Acad. Sci. USA.* 19:7273–7277.
23. Acker, G. W., and R. L. Steere. 1962. Restricted diffusion of macromolecules through agar-gel membranes. *Biochim. Biophys. Acta.* 59:137–149.
24. Rigler, R., and M. Ehrenberg. 1973. Molecular interactions and structures as analysed by fluorescence relaxation spectroscopy. *Q. Rev. Biophys.* 6:139–199.
25. Kawato, S., and K. Kinosita, Jr. 1981. Time-dependent absorption anisotropy and rotational diffusion of proteins in membranes. *Biophys. J.* 36:277–296.
26. Albrecht, A. C. 1970. The method of photoselection and some recent applications. *Prog. React. Kinet.* 5:301–334.
27. Albrecht, A. C. 1961. Polarizations and assignments of transitions: the method of photoselection. *J. Mol. Spectrosc.* 6:84–108.
28. Weber, G. 1953. Rotational brownian motion and polarization of the fluorescence of solutions. *Adv. Protein Chem.* 8:415–459.
29. Kouyama, T., Y. Kimura, K. Kinosita, Jr., and A. Ikegami. 1981. Immobility of the chromophore in bacteriorhodopsin. *FEBS (Fed. Eur. Biochem. Soc.). Lett.* 124:100–104.
30. Huang, K-S, R. Radhakrishnan, H. Bayley and H. G. Khorana. 1982. Orientation of retinal in bacteriorhodopsin as studied by cross-linking using a photosensitive analog of retinal. *J. Biol. Chem.* 257:1316–1323.
31. Treuhella, J., S. Anderson, R. Fox, E. Gogol, S. Khan, D. Engelman, and G. Zaccai. 1983. Assignment of segments of the bacteriorhodopsin sequence to positions in the structural map. *Biophys. J.* 42:233–241.
32. Cherry, R. J., and R. E. Godfrey. 1981. Anisotropic rotation of bacteriorhodopsin in lipid membranes. Comparison of theory with experiment. *Biophys. J.* 36:257–276.
33. Hwang, S. B., R. A. Bogomolni, Y. W. Tseng, and W. Stoeckenius. 1977. Angular orientation of an intermediate of the bacteriorhodopsin photochemical reaction cycle. *Biophys. J.* 17:98*a*.
34. Korenstein, R., and B. Hess. 1978. Immobilization of bacteriorhodopsin and orientation of its transition moment in the purple membrane. *FEBS* (*Fed. Eur. Biochem. Soc.*). *Lett.* 89:15–20.
35. Tokutomi, S., I. Tatsuo, T. Yoshizawa, and S-I. Ohnishi. 1981. Flash-induced fast change in surface potential and fluidity of purple membranes studied by spin label method. *Photochem. Photobiol.* 33:467–474.
36. Frankel, R. D., and J. M. Forsyth. 1982. Time resolved x-ray diffraction studies on purple membranes from *Halobacterium halobium*. *Biophys. J.* 37(2, Pt. 2):232*a*. (Abstr.)
37. Dencher, N. A., and M. P. Heyn. 1979. Bacteriorhodopsin monomers pump protons. *FEBS* (*Fed. Eur. Biochem. Soc.*). *Lett.* 108:307–310.
38. Eisenbach, M., C. Weissmann, G. Tanny, and S. R. Caplan. 1977. Bacteriorhodopsin-loaded charged synthetic membranes. *FEBS* (*Fed. Eur. Biochem. Soc.*). *Lett.* 81:77–80.